IRSTI 31.15.33
Section: Chemistry
Article

Facile thermal oxidation and carbon coating strategy for fabricating a 3D Zn/ZnO@C anode

Yerzhigit Serik[1,2], Nurbolat Issatayev[3], Moldir Arkharbekova[1,2], Zhumabay Bakenov[1,3,4], Arailym Nurpeissova[1,4], Aliya Mukanova[1,4*]

[1]National Laboratory Astana, Kazakhstan, nla@nu.edu.kz
[2]Department of Chemistry, Eurasian National University, Astana, Kazakhstan, enu@enu.kz
[3]Department of Chemical and Materials Engineering, School of Engineering and Digital Sciences, Nazarbayev University, Astana, Kazakhstan, nu@old.nu.edu.kz
[4]Institute of Batteries, Astana, Kazakhstan
*Correspondence: aliya.mukanova@nu.edu.kz

Abstract: With the increasing demand for efficient and environmentally friendly energy storage, developing alternatives to commercial graphite anodes in lithium-ion batteries (LIBs) has become a major research focus. Zinc oxide (ZnO) is a promising candidate due to its high theoretical capacity (978 mAh/g), but its practical application is limited by large volume expansion, low electrical conductivity, and poor cycling stability. In this study, a three-dimensional (3D) Zn/ZnO foam was synthesized via thermal oxidation and then coated with carbon through carbonization of polyethylene oxide (PEO). The 3D porous structure facilitates ion and electron transport, while the carbon coating mitigates volume changes during cycling and enhances overall conductivity. Structural and chemical analyses using XRD, SEM, SEM-EDS, and FTIR confirmed the successful fabrication of the Zn/ZnO@C composite. Electrochemical tests showed that Zn/ZnO@C maintained a specific capacity of approximately 380 mAh/g after 100 cycles at a current density of 50 mA/g, compared to only 100 mAh/g for the uncoated Zn/ZnO sample. This significant improvement in performance highlights the potential of carbon-coated Zn/ZnO foam as a high-performance anode material for next-generation lithium-ion batteries.

Keywords: lithium-ion batteries; electrode materials; energy storage systems; electrochemistry

Citation: Serik, Y., Issatayev, N., Arkharbekova, M., Bakenov, Z., Nurpeissova, A., Mukanova, A. (2025). Facile Thermal Oxidation and Carbon Coating Strategy for Fabricating a 3D Zn/ZnO@C Anode. Bulletin of the L.N. Gumilyov ENU. Chemistry. Geography. Ecology Series, 152(3), 92-105. https://doi.org/10.32523/2616-6771-2025-152-3-92-105

Academic Editor:
E.Ye. Kopishev

Received: 06.08.2025
Revised: 30.08.2025
Accepted: 01.09.2025
Published: 30.09.2025

1. Introduction

The substantial rise in fossil fuel consumption over the past two decades for electricity generation has emerged as a major contributor to global ecological degradation, including greenhouse gas emissions, climate change, and air pollution. As a result, the global energy landscape is undergoing a transformation toward sustainable and environmentally friendly alternatives. Renewable energy technologies, particularly solar and wind power, have been increasingly adopted to address these challenges. However, these sources are inherently intermittent and

location-dependent, necessitating the development of efficient, reliable, and scalable energy storage systems to ensure a stable power supply and grid integration (Cai et al., 2020).

Among the various energy storage technologies available, lithium-ion batteries (LIBs) have garnered considerable attention due to their high energy density, long cycle life, low self-discharge, and relatively high efficiency. These characteristics have made LIBs indispensable in applications ranging from portable electronics to electric vehicles and grid-level storage systems. However, the demand for high-performance batteries continues to increase, prompting the need for further improvements in specific capacity, rate capability, and cycling stability (Hao et al., 2020; Tarascon & Armand, 2001).

Conventional LIB anodes, particularly those based on two-dimensional (2D) electrode structures and commercial graphite, are reaching their theoretical performance limits. Graphite anodes offer a theoretical capacity of only 372 mAh/g, which restricts the energy density of LIBs. Attempts to increase electrode mass loading often lead to thicker electrodes with prolonged ion diffusion paths and higher internal resistance, ultimately degrading the battery's rate performance and fast-charging ability (Y. Liu et al., 2019). To address these challenges, three-dimensional (3D) structured current collectors and electrode architectures have emerged as a promising design strategy. The 3D porous framework offers a high surface area for active material deposition, facilitates electrolyte infiltration, shortens ion/electron transport pathways, and accommodates volume expansion during cycling, thereby enhancing both energy and power performance (Zhang et al., 2017).

In pursuit of higher-capacity anode materials, transition metal oxides (TMOs) have attracted significant attention due to their abundance, environmental benignity, and high theoretical capacities. Materials such as CuO (674 mAh/g), NiO (718 mAh/g), and particularly ZnO (978 mAh/g) have been widely investigated as potential anode candidates (Issatayev, Adylkhanova, et al., 2024; Issatayev et al., 2021). Among these, ZnO stands out for its high theoretical capacity, low cost, nontoxicity, and chemical stability. However, ZnO-based anodes face several critical challenges, including low intrinsic electrical conductivity, sluggish lithium-ion diffusion kinetics, and substantial volume expansion (~300%) during lithiation/delithiation processes. These drawbacks often result in mechanical degradation, particle pulverization, and rapid capacity fading upon cycling (Khac et al., 2021).

To mitigate these limitations, researchers have developed various strategies, among which carbon coating has emerged as one of the most effective approaches. Carbonaceous materials, such as graphene, carbon nanotubes, and amorphous carbon, serve as conductive matrices or protective layers that enhance electronic conductivity, buffer volume changes, and prevent direct contact between ZnO and electrolyte, thereby minimizing side reactions and stabilizing the solid electrolyte interphase (SEI) layer (Y. Liu et al., 2019). For instance, Thauer et al. (2023) reported ZnO/C composites prepared via the calcination of zinc glycerolate under nitrogen, achieving a specific capacity of 212 mAh/g compared to 100 mAh/g for bare ZnO at a current density of 100 mA/g (Thauer et al., 2021a). Bai et al. (2013) synthesized ZnO@C nanospheres via a one-step co-pyrolysis of zinc and acetylacetone, yielding a carbon-coated structure, demonstrating enhanced electrochemical stability (Bai et al., 2014). Recent studies have also highlighted the effectiveness of hydrothermal synthesis and annealing techniques in developing ZnO nanorods coated with carbon, achieving improved capacity retention and structural integrity (Ding et al., 2019).

Further improvements can be achieved by combining carbon coating with 3D current collector designs. In this context, metal foams - such as copper or zinc foams - offer a self-supporting, conductive, and porous scaffold for growing active materials. When combined with a carbon layer, the resulting 3D hybrid structures exhibit synergistic effects: the foam provides structural robustness and continuous electron pathways, while the carbon coating ensures surface passivation and conductivity. This dual-function approach provides a viable pathway for achieving high-performance ZnO-based anodes (Issatayev et al., 2021).

Building on these recent advances, the present study introduces a novel 3D Zn/ZnO@C foam electrode synthesized through a simple and scalable two-step process. In the first step, commercial

Zn foam is thermally oxidized to form a conformal ZnO layer. Subsequently, the Zn/ZnO composite is coated with polyethylene oxide (PEO) via dip-coating and subjected to carbonization under an argon atmosphere. PEO serves as the carbon precursor, producing a thin, uniform carbon layer upon pyrolysis. This carbon layer not only enhances electronic conductivity but also provides mechanical stability during cycling. The 3D foam structure offers improved electrolyte accessibility and reduced ion diffusion resistance, contributing to superior electrochemical kinetics. Electrochemical evaluation revealed that the Zn/ZnO@C foam exhibited significantly enhanced performance compared to uncoated Zn/ZnO foam, delivering a reversible capacity of approximately 380 mAh/g after 100 cycles at 100 mA/g. The results of this work underscore the effectiveness of integrating carbon coating and 3D architecture for developing high-performance ZnO-based anodes for next-generation lithium-ion batteries.

2. Materials and methods

2.1 Materials

Zn foam deposited in Ni foam was purchased from DEK Research. Polyethylene oxide (PEO, average M_w = 100000) and Acetonitrile were purchased from Sigma Aldrich. The authors used OpenAI's ChatGPT (GPT-4, accessed via chat.openai.com) as a language support tool to assist with academic writing, grammar refinement, and paraphrasing, and for generating the animated 3D structure of Zn foam and modified electrodes. No data or results were generated by the AI; all scientific input, analysis, and interpretation were solely the responsibility of the authors.

2.2 Synthesis of Zn/ZnO foam

The porous ZnO electrodes were fabricated by thermal oxidation of pure Zn foam (0.5 mm thickness, 95-98% porosity) in air using a muffle furnace. At first, Zn foam was cut into disks with a 14 mm diameter. Cut disks were cleaned by ultrasonication in a solution of ethanol and acetone in the ratio of 1:1 to remove dust and dirt. After the cleaning process, the washed disks were dried in a vacuum oven at 60°C for 3 h to completely dry any moisture. After all of these preparation processes, Zn foams were placed into a muffle furnace to 500°C for 15 minutes at a controlled rate of 5°C per minute. As a result of thermal oxidation, Zn/ZnO foams were obtained. The average mass of the ZnO coating was approximately 8–10 mg**.**

2.3 Synthesis of Zn/ZnO@C foam

The carbon layer was obtained by dip coating the Zn/ZnO foam into a 15% solution of PEO. After each dipping, polymer-coated Zn/ZnO foam was dried at 50°C in a drying oven for 30 minutes with ventilation turned off. This dip coating process was repeated several times to ensure a uniform polymer coating. Finally, the obtained polymer-coated Zn/ZnO foam was annealed at 600°C for 1h in an argon atmosphere, with a ramping rate of 5°C per minute. To investigate the effect of carbon coating on the electrochemical performance of Zn/ZnO foam anode, the polymer coating was applied in 5 and 7 layers.

2.4 Material Characterization

The structural characterization of the obtained materials was performed by X-ray diffraction (XRD) using a MiniFlex 600/600-C Benchtop X-ray diffractometer (Rigaku, Japan) covering diffraction angles from 25° to 95° at a scanning rate of 5° per minute. Scanning electron microscopy (SEM, JEOL JSM-IT800, Japan) coupled with energy-dispersive X-ray spectroscopy (EDS) was used to examine film morphologies.

2.5 Electrochemical measurements

The electrochemical performance of the samples was investigated using CR2032 coin-type batteries assembled in an argon-filled glove box (MBRAUN, LABmaster PRO Glovebox, Germany) containing <0.1 ppm O_2 and <0.1 ppm H_2O. Lithium chips are used as an opposite and reference electrode. The lithium hexafluorophosphate ($LiPF_6$) dissolved in a mixture of ethylene carbonate

(EC), diethyl carbonate (DEC), and ethyl methyl carbonate (EMC) in a volume ratio of 1:1:1 was utilized as an electrolyte. Celgard 2400, microporous polypropylene, was employed as the separator membrane. After assembly, the coin cells were kept overnight, and following this rest, they were tested on a Neware BTS4000 test (Neware Co., Shenzhen, China) system across a potential range of 0.05 to 2.5 V vs. Li/Li^+. The mass of ZnO and carbon in the Zn/ZnO@C foam is utilized for calculating the current. Current density was calculated using the total mass of ZnO and carbon (6–8 mg).

3. Results

According to the conducted research, the morphological and electrochemical analyses were done and demonstrated in subsection 3.1. Meanwhile, the chemical equations provided in subsection 3.2 and discussed in section 4.

3.1. Figures and Schemes

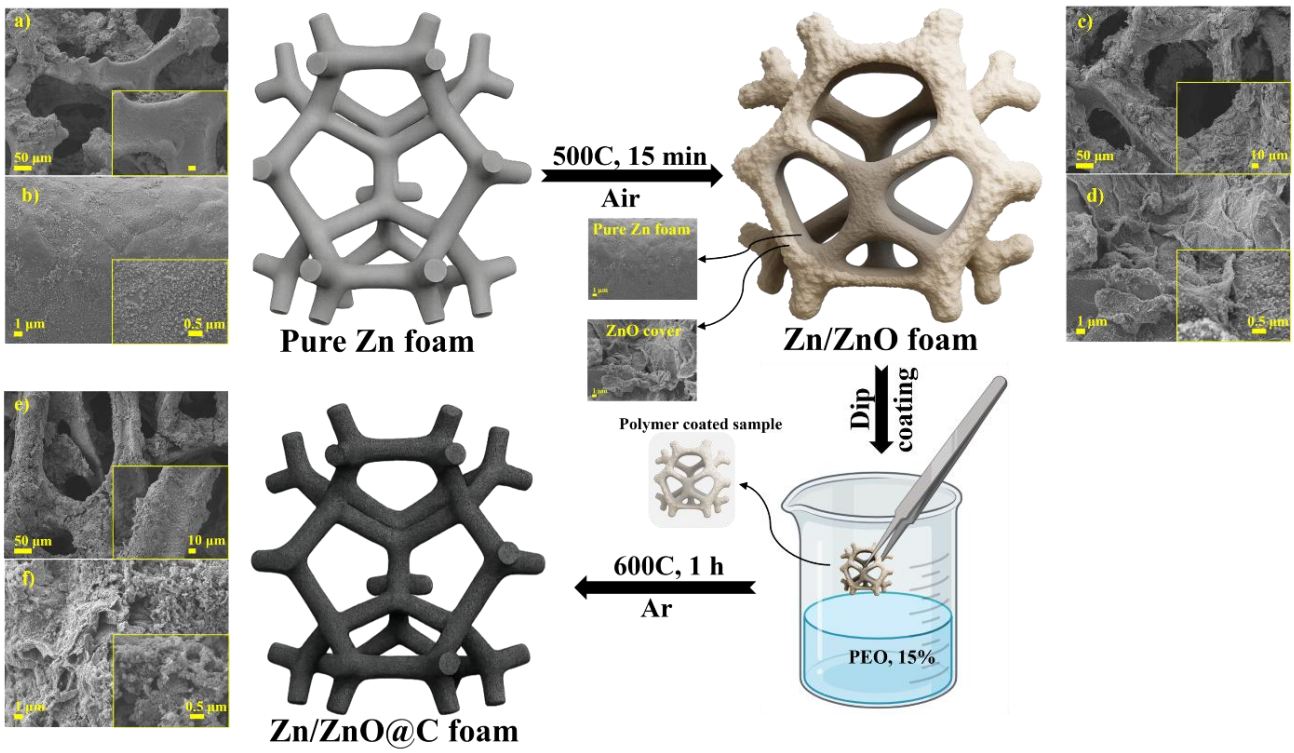

Figure 1. Experimental part illustration and SEM images at various magnifications: a-b) Zn foam, c-d) Zn/ZnO foam, e-f) Zn/ZnO@C foam

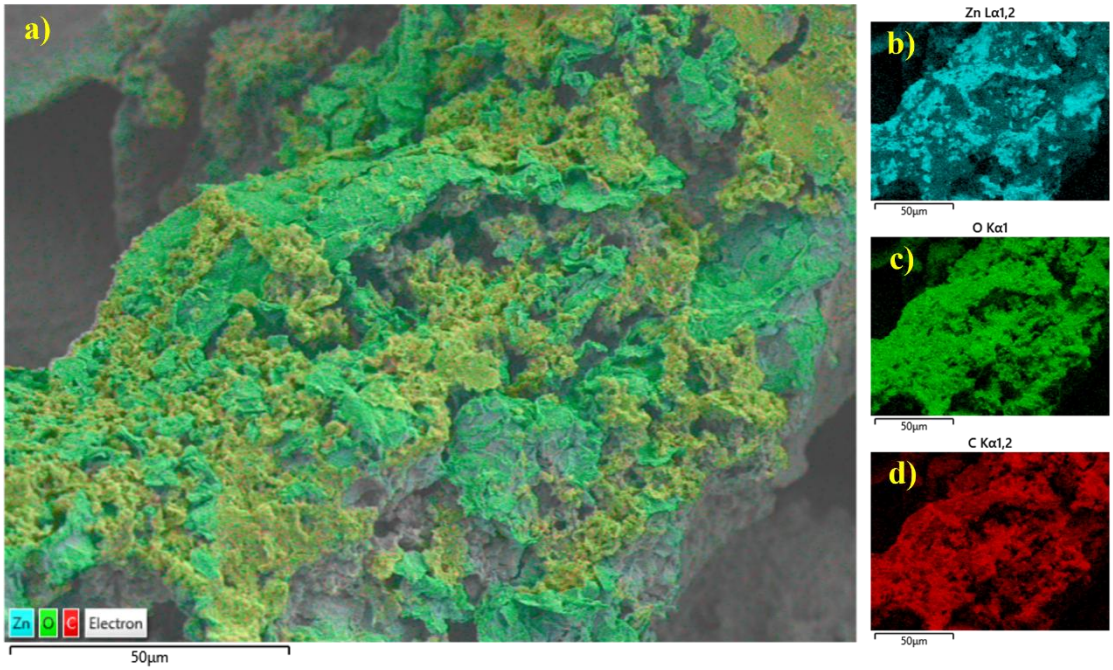

Figure 2. EDS mapping of Zn, O, and C elements on the surface of Zn/ZnO@C foam

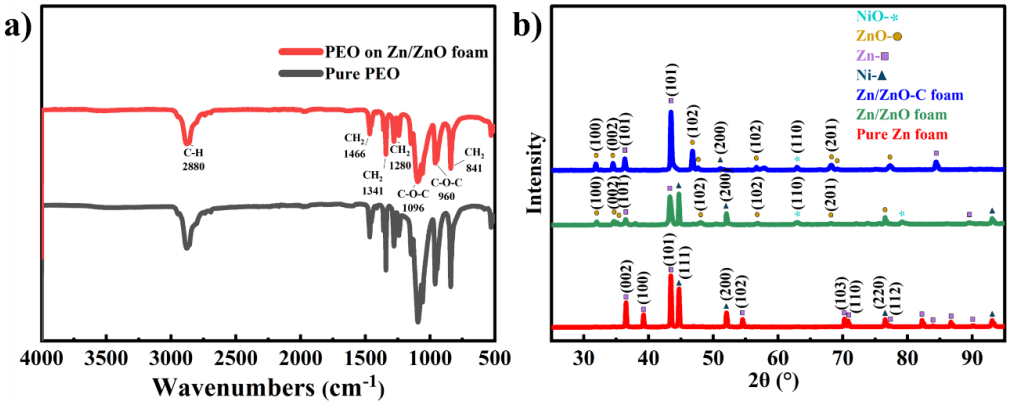

Figure 3. a) FTIR spectra of pure PEO and coated on Zn/ZnO foam; b) XRD patterns of pure Zn foam, Zn/ZnO foam, and Zn/ZnO-C foam

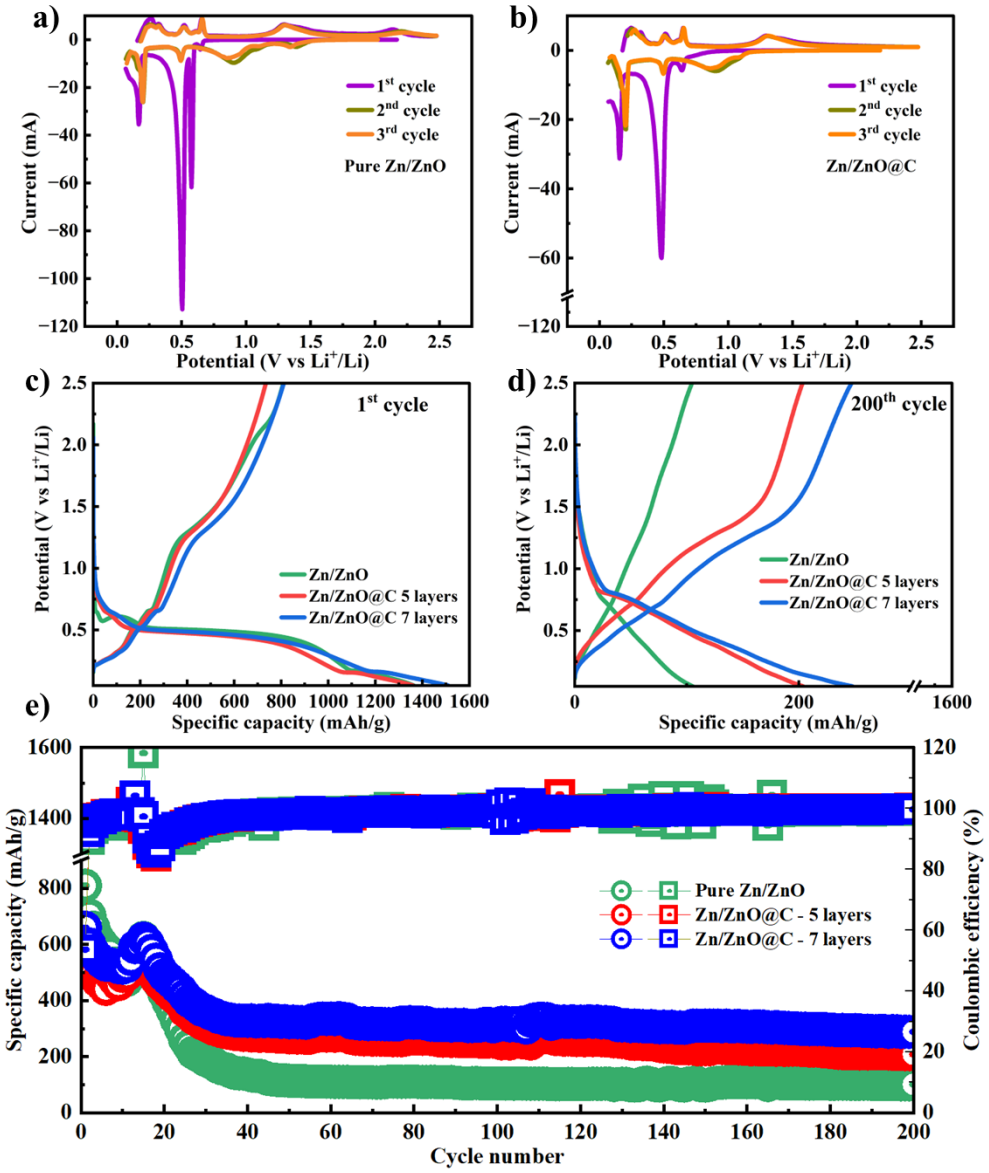

Figure 4. dQ/dV plots of **(a)** pure Zn/ZnO foam and **(b)** Zn/ZnO@C foam and potential profiles of all electrodes at **(c)** the 1st cycle and **(d)** 100th cycle at the current density of 50 mA/g. **(e)** Cycle performance of all synthesized electrodes

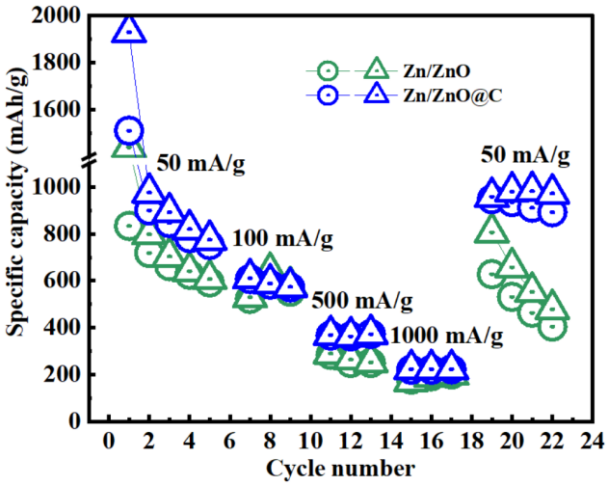

Figure 5. The rate capability of Zn/ZnO foam and Zn/ZnO@C foam

3.2 Chemical Equations

$$yZn + xLi^+ + x\bar{e} = Li_xZn_y \quad (1)$$
$$ZnO + 2Li^+ + 2\bar{e} = Zn + Li_2O \quad (2)$$
$$NiO + 2Li^+ + 2\bar{e} = Ni + Li_2O \quad (3)$$
$$Zn + Li_2O = ZnO + 2Li^+ + 2\bar{e} \quad (4)$$
$$Ni + Li_2O = NiO + 2Li^+ + 2\bar{e} \quad (5)$$

4. Discussion

The Zn/ZnO–C foam was synthesized via a straightforward two-step process, as illustrated in Fig. 1. In the first step, pure Zn foam underwent thermal oxidation to develop a conformal ZnO layer on its surface. This was followed by a dip-coating procedure using a polyethylene oxide (PEO) solution and subsequent carbonization in a tube furnace under an argon atmosphere. Here, PEO acted as the carbon source, enabling the formation of a uniform carbon coating on the Zn/ZnO surface. This carbon layer is crucial, as it enhances the electronic conductivity of the electrode and helps stabilize its electrochemical behavior by mitigating volume changes during lithium cycling.

To evaluate the morphological evolution throughout each synthesis stage, scanning electron microscopy (SEM) was conducted on the pristine Zn foam, oxidized Zn/ZnO foam, and carbon-coated Zn/ZnO@C foam (Fig. 1). The SEM images of the untreated Zn foam reveal a highly porous, three-dimensional architecture composed of interconnected pores, which provides a large surface area beneficial for ion transport and subsequent surface modification. At low magnification, variations in topography were noted - some regions appeared smooth, while others showed a degree of roughness. High-magnification images further disclosed the presence of fine particles, likely corresponding to a thin native oxide layer formed from atmospheric exposure.

Following thermal oxidation, a significant transformation in surface morphology was observed. The Zn/ZnO foam exhibited increased roughness and surface complexity, confirming the formation of ZnO. SEM images indicated that the metal surface was uniformly covered with nanoscale ZnO particles, forming a dense and adherent oxide film. The absence of microcracks or delamination reflects good mechanical integrity of the oxide layer, a critical factor for long-term cycling stability.

In the final modification stage, the Zn/ZnO foam underwent multiple dip-coating cycles in a 15 wt% PEO solution, followed by carbonization. This resulted in the formation of Zn/ZnO@C foam with a well-distributed carbon layer. High-magnification SEM images revealed a further increase in surface texture, indicative of successful carbon deposition. The coating appeared to be continuous, porous, and uniformly spread across the foam framework. The uniformity and presence of porosity were confirmed through SEM at different magnifications, which demonstrated continuous coverage without cracks or agglomerations, while SEM–EDS mapping (Fig. 2) further verified the homogeneous distribution of carbon and oxygen signals. The porous nature of the coating was supported by nanoscale voids observed in high-magnification SEM images, typical for polymer-derived carbons after pyrolysis (Thauer et al., 2021; Zhang et al., 2018). Although layer thickness and specific surface area were not directly quantified, these morphological observations strongly indicate a uniform and porous coating.

To support these morphological findings, elemental mapping was performed using SEM–EDS analysis (Fig. 2). The oxygen distribution map (Fig. 2c) confirmed the successful formation of a ZnO layer via thermal oxidation. Simultaneously, carbon mapping (Fig. 2d) validated the presence of a uniform carbon layer formed during PEO carbonization. It should be noted that the oxygen detected in EDS mapping originates from ZnO, NiO (formed via partial oxidation of the Ni substrate), and residual oxygen-containing groups in the carbon.

The structural evolution of the materials was further characterized by X-ray diffraction (XRD), as shown in Fig. 2b. The XRD pattern of pristine Zn foam exhibited sharp diffraction peaks at 36.5°, 39.2°, 43.5°, 54.4°, 70.3°, 70.8°, and 77.1°, corresponding to the (002), (100), (101), (102), (103), (110), and (112) planes of metallic Zn, respectively (Chou et al., 2019; Lin et al., 2012; Pramanik et al., 2023). Additionally, peaks at 44.8°, 52.1°, and 76.6° matched the (111), (200), and (220) planes

of Ni, confirming the Ni substrate underneath the Zn coating, consistent with the SEM observations (Srinivasa et al., 2021).

Following thermal oxidation and carbonization, new peaks emerged at 32.1°, 34.7°, 35.2°, 48.1°, 56.8°, 68.1°, and 76.6°, indexed to the (100), (002), (102), (102), (201), (110), and (112) planes of ZnO, which confirm the successful synthesis of ZnO (Ghosh & Raychaudhuri, 2008). Furthermore, peaks at 63.1° and 79.1°, corresponding to the (200) and (222) planes of NiO, were also detected, indicating partial oxidation of the Ni substrate during the thermal treatment step (Rahdar et al., 2015; Song et al., 2022).

To confirm the presence of the PEO-derived carbon coating, Fourier-transform infrared spectroscopy (FTIR) was conducted on the polymer-coated samples (Fig. 3a). The spectrum showed a prominent peak at 2877 cm^{-1}, corresponding to the asymmetric C–H stretching of methylene groups—a signature of pure PEO (Abdelrazek et al., 2018). Additionally, characteristic CH_2 wagging vibrations appeared at 1341 cm^{-1} and 1467 cm^{-1}. A cluster of strong bands around 1092 cm^{-1}, accompanied by peaks at 1145 cm^{-1} and 1060 cm^{-1}, was assigned to the C–O–C stretching vibrations, with the 1092 cm^{-1} band being the most intense (Arinova et al., 2023). Minor peaks at 960 cm^{-1} and 841 cm^{-1} were attributed to asymmetric rocking motions of CH_2, while the absorption band at 531 cm^{-1} corresponded to C–O–C bending(Kumar et al., 2014; Tleukenov et al., 2022). These FTIR results support the successful deposition of a PEO-derived carbonaceous layer on the Zn/ZnO surface. The oxygen functionalities observed in the carbon layer arise from decomposition of PEO during carbonization and partial contribution from ZnO. Their concentration was effectively controlled by carbonization at 600°C under Ar, which removed most oxygen-containing groups while retaining a fraction of stable residual functionalities. This selective removal enhances conductivity while limited residual oxygen improves interfacial wettability and ion transport. Although these groups were not quantitatively measured in our study, the improved conductivity and stable cycling performance of the Zn/ZnO@C electrode are consistent with prior reports on ZnO/C composites where oxygen functionalities were analyzed by XPS (Thauer et al., 2021; Bui et al., 2021; Zhang et al., 2018).

Figures 4a and 4b present the differential capacity (dQ/dV) curves for the bare Zn/ZnO foam and the Zn/ZnO–C foam, respectively. For the pristine Zn/ZnO foam, the cathodic scan reveals a distinct peak at approximately 0.1 V, which corresponds to the alloying reaction between Zn and Li^+, as described by Eq. 1 (Belliard & Irvine, n.d.). A prominent peak observed at around 0.5 V is attributed to the formation of the solid electrolyte interphase (SEI), a typical feature of the initial lithiation cycle (Belliard & Irvine, n.d.). Additionally, a strong reduction peak at 0.65 V is associated with the conversion reaction of ZnO with Li^+ ions (Eq. 2) (J. Liu et al., 2008). Since the ZnO layer was formed by thermal oxidation on Zn-coated Ni foam, the presence of NiO is also expected and was confirmed through XRD and SEM analyses. A smaller peak at 0.58 V corresponds to the reduction of NiO to metallic Ni, as represented by Eq. 3 (Issatayev, Abdumutaliyeva, et al., 2024).

As the electrochemical cycling progresses, structural and morphological changes - such as electrolyte decomposition—cause a shift of these cathodic peaks to higher potentials in subsequent cycles. During the anodic scan, multiple peaks appear at 0.27 V, 0.3 V, 0.52 V, and 0.65 V, which are indicative of a multi-step dealloying process of the Li-Zn alloy (Gachot et al., 2008; Huang et al., 2011; N. Li et al., 2014; Shen et al., 2013). Additionally, anodic peaks at approximately 1.2 V and 2.1 V correspond to the reversible reformation of ZnO and NiO, respectively, as represented by Eq. 4 and 5 (Issatayev, Abdumutaliyeva, et al., 2024; N. Li et al., 2014).

Interestingly, in the differential capacity (dQ/dV) profile of the Zn/ZnO–C electrode (Fig. 4b), peaks attributed to NiO are no longer observed, which contrasts with the pure Zn/ZnO foam. This absence suggests that the NiO component does not actively participate in electrochemical reactions with Li^+ ions, likely due to passivation by the carbon coating. Nonetheless, the remaining peaks closely resemble those seen in the uncoated sample, thereby confirming the electrochemical inertness of the carbon layer and its non-involvement in redox processes (Issatayev, Abdumutaliyeva, et al., 2024).

This interpretation is further supported by the potential–capacity profiles at a current density of 50 mA g^{-1}, shown in Figures 4c and 4d, which are consistent with the dQ/dV features described

above. As commonly observed in conversion-type electrodes, the initial discharge capacities of all samples were noticeably higher than those recorded in subsequent cycles, a behavior attributed to SEI formation. Specifically, the initial charge/discharge capacities of Zn/ZnO, Zn/ZnO@C-5, and Zn/ZnO@C-7 were 809/1363 mAh g^{-1}, 734/1361 mAh g^{-1}, and 810/1510 mAh g^{-1}, respectively. The corresponding initial coulombic efficiencies (ICE) were 59% for bare Zn/ZnO and 54% for both carbon-coated samples. These lower ICE values in carbon-coated electrodes are attributed to their higher surface area, which increases active sites for electrolyte decomposition and SEI formation. SEM/EDS and porous morphology support this, consistent with previous reports linking higher surface areas and oxygen groups to larger irreversible capacities (Thauer et al., 2021).

The lower ICE values in the carbon-coated electrodes are most likely due to their higher specific surface areas, which increase the number of active sites available for electrolyte decomposition and SEI formation. As a result, more Li^+ ions are irreversibly consumed during the initial cycle, contributing to the lower coulombic efficiency.

Despite this early inefficiency, the long-term cycling results indicate that carbon-coated samples achieve significantly improved stability. By the 100th cycle, the Zn/ZnO, Zn/ZnO@C-5, and Zn/ZnO@C-7 electrodes-maintained charge/discharge capacities of 104/105 mAh g^{-1}, 317/320 mAh g^{-1}, and 383/389 mAh g^{-1}, respectively. Moreover, their coulombic efficiencies improved to 99.3%, 99.2%, and 98.4%, indicating that the lithiation/delithiation processes became highly reversible over extended cycling.

To further explore this long-term stability, the cycling performance was evaluated at a current density of 50 mA g^{-1} across a voltage range of 0.05–2.5 V, as shown in Fig. 4e. The data reinforces the superior capacity retention of carbon-coated samples compared to the bare Zn/ZnO electrode. After 100 cycles, the Zn/ZnO sample maintained a specific capacity of ~100 mAh g^{-1}, while Zn/ZnO@C-5 and Zn/ZnO@C-7 retained ~320 mAh g^{-1} and ~380 mAh g^{-1}, respectively.

All electrodes initially exhibited a decrease in capacity over the first 20 cycles, which can be attributed to the ~300% volume expansion of ZnO during lithiation/delithiation. This significant expansion impairs the mechanical integrity of the electrode, leading to layer cracking and loss of active material. However, following this initial degradation, a moderate increase in specific capacity was observed, likely due to the exposure of new electrochemically active sites formed because of structural fracturing. Eventually, with prolonged cycling, mechanical degradation reaches a critical point beyond which capacity undergoes irreversible fading.

The presence of a carbon coating plays a crucial role in mitigating this issue. Owing to its electrical conductivity and structural flexibility, the carbon layer effectively suppresses the negative impact of volume fluctuations, thereby enhancing the cycling stability. Notably, this improvement is attributed to the mechanical buffering effect of the carbon rather than its electrochemical activity. This is further supported by the absence of any carbon-related peaks in the differential capacity (dQ/dV) profiles, indicating that the carbon does not participate in redox reactions within the cell (Wang et al., 2022).

As shown in Fig. 5, the discharge capacities of Zn/ZnO@C foam at current densities of 50, 100, 500, and 1000 mA g^{-1} were 1929, 615, 371, and 225 mAh g^{-1}, respectively. When the current was reduced back to 50 mA g^{-1}, the capacity quickly recovered to 964 mAh g^{-1}, demonstrating excellent rate reversibility and structural integrity. In contrast, the pristine Zn/ZnO foam delivered lower discharge capacities of 1445, 533, 292, and 174 mAh g^{-1} at the same respective current densities, and showed a lower recovery capacity of 811 mAh g^{-1} when returned to 50 mA g^{-1}. The performance degradation observed in Zn/ZnO foam can be attributed to increased internal resistance and structural instability under rapid charge/discharge cycling, which may lead to mechanical degradation and loss of electrochemical active sites. By comparison, the good electrochemical performance of Zn/ZnO@C foam is ascribed to the uniform carbon coating that enhances electronic conductivity and suppresses volume expansion during lithiation/delithiation. This buffering effect not only preserves the electrode's structural integrity but also facilitates ion/electron transport, resulting in higher specific capacities, improved rate capability, and good reversibility. These results confirm that the

introduction of carbon significantly improves the electrochemical kinetics and mechanical stability of Zn/ZnO-based electrodes for lithium-ion batteries (Thauer et al., 2021a).

To benchmark our approach, Table 1 compiles ZnO-based electrodes coated with carbon from different precursors alongside their electrochemical metrics, providing direct context that our PEO-derived Zn/ZnO@C foam delivers competitive or superior performance.

Table 1. Comparison of ZnO-based anodes with carbon coatings from different precursors.

Sample	Carbon Source / Coating Method	Capacity After 100 Cycles (mAh/g)	Current Density	Bare ZnO after 100 cycles (mAh/g)	DOI / Reference
ZnO/C (from zinc glycerolate)	Calcination of zinc glycerolate in N_2	300	100 mA/g	100	(Thauer et al., 2021b)
ZnO/C microspheres	Sol-gel + calcination	490	100 mA/g	360	(Guo et al., 2020)
ZnO/C	Atomic layer deposition	430	200 mA/g	200	(Y. Li et al., 2017)
ZnO/C microspheres	ZnO nanorods coated with carbon nanotubes	330 (50 cycles)	0.25C	-	(J. Liu et al., 2009)
Zn/ZnO@C foam (coated)	Dip coating with PEO + pyrolysis	380	50 mA/g	100	This work

5. Conclusion

In summary, a carbon-coated Zn/ZnO anode was successfully fabricated on Zn foam via thermal oxidation followed by carbonization, and demonstrated as a three-dimensional (3D) structured material for lithium-ion batteries (LIBs). Structural and compositional analyses using XRD, SEM, SEM–EDS, and FTIR confirmed the successful formation of the carbon-coated ZnO on the 3D foam substrate. The interconnected porous architecture provided a high surface area that enhanced electrolyte accessibility and shortened lithium-ion diffusion paths. Additionally, the carbon layer effectively buffered the large volume changes of ZnO during cycling and improved its intrinsic electronic conductivity. As a result, the Zn/ZnO@C electrode delivered significantly improved electrochemical performance, achieving a stable capacity of approximately 380 mAh g^{-1} at 50 mA g^{-1} after 100 cycles, compared to only ~100 mAh g^{-1} for the uncoated Zn/ZnO electrode under the same conditions. This substantial enhancement highlights the potential of carbon-coated Zn/ZnO foams as promising anode materials for next-generation high-performance LIBs.

6. Supplementary Materials: No supplementary materials.

7. Author Contribution:

Author Contributions: Conceptualization - A.N., A.M.; methodology – A.N., N.I.; software, - Y.S.; validation - Y.S., M.A., Z.B.; formal analysis - Z.B., A.N., A.M.; investigation - Y.S., M.A.; resources - Z.B., A.N., A.M.; data curation - Y.S., M.A.; writing - original draft preparation - Y.S., N.I.; writing - review and editing - N.I., Z.B., A.N., A.M.; visualization - Y.S., N.I., M.A.; supervision - N.I., A.N., A.M.; project administration - A.M.; funding acquisition - A.N., A.M. All authors have read and agreed to the published version of the manuscript.

8. Author Information:

Serik, Yerzhigit - research assistant, National Laboratory Astana, Kabanbay Batyr Ave. 53, Astana, Kazakhstan. Department of Chemistry, Eurasian National University, Satpayev St. 2, Astana, Kazakhstan, 010000; email: yerzhigit.serik@nu.edu.kz, https://orcid.org/0009-0002-0222-9872

Issatayev, Nurbolat - researcher, Department of Chemical and Materials Engineering, School of Engineering and Digital Sciences, Nazarbayev University, Kabanbay Batyr Ave. 53, Astana, Kazakhstan, 010000; nurbolat.issatayev@nu.edu.kz, https://orcid.org/0000-0003-4988-4014

Arkharbekova, Moldir - research assistant, National Laboratory Astana, Kabanbay Batyr Ave. 53, Astana, Kazakhstan. Department of Chemistry, Eurasian National University, Satpayev St. 2, Astana, Kazakhstan, 010000; email: moldir.arkharbekova@nu.edu.kz, https://orcid.org/0009-0002-4939-3645

Bakenov, Zhumabay - Professor, National Laboratory Astana, Kabanbay Batyr Ave. 53, Astana, Kazakhstan. Department of Chemical and Materials Engineering, School of Engineering and Digital Sciences, Nazarbayev University, Kabanbay Batyr Ave. 53, Astana, Kazakhstan. Institute of Batteries, Kabanbay Batyr Ave. 53, Astana, Kazakhstan, 010000; email: Zbakenov@nu.edu.kz, https://orcid.org/0000-0003-2781-4955

Nurpeissova, Arailym - leading researcher, National Laboratory Astana, Kabanbay Batyr Ave. 53, Astana, Kazakhstan. Institute of Batteries, Kabanbay Batyr Ave. 53, Astana, Kazakhstan, 010000; email: arailym.nurpeissova@nu.edu.kz, https://orcid.org/0000-0002-9657-2964

Mukanova, Aliya - leading researcher, National Laboratory Astana, Kabanbay Batyr Ave. 53, Astana, Kazakhstan. Institute of Batteries, Kabanbay Batyr Ave. 53, Astana, Kazakhstan, 010000; email: aliya.mukanova@nu.edu.kz, https://orcid.org/0000-0002-1171-176X

9. Funding: This research is funded by the Science Committee of the Ministry of Science and Higher Education of the Republic of Kazakhstan (Grant No. AP19578472 and BR21882402).

10. Acknowledgements: The authors would like to express their gratitude to the Core Facility of Nazarbayev University for granting access to the characterization equipment.

11. Conflicts of interest: The authors declare no conflicts of interest.

12. References

1. Abdelrazek, E.M., Abdelghany, A.M., Badr, S.I., Morsi, M.A. (2018). Structural, optical, morphological and thermal properties of PEO/PVP blend containing different concentrations of biosynthesized Au nanoparticles. *Journal of Materials Research and Technology* 7(4), 419–431. https://doi.org/10.1016/j.jmrt.2017.06.009
2. Arinova, A., Kalimuldina, G., Nurpeissova, A., Bakenov, Z. (2023). Electrophoretic Deposition of Poly(ethylene oxide) Gel-Polymer Electrolyte for 3D NiO/Ni Foam Anode Based Lithium-Ion Batteries. *Journal of The Electrochemical Society* 170(10), 100501. https://doi.org/10.1149/1945-7111/acfe3e
3. Bai, Z., Zhang, Y., Fan, N., Guo, C., Tang, B. (2014). One-step synthesis of ZnO@C nanospheres and their enhanced performance for lithium-ion batteries. *Materials Letters* 119, 16–19. https://doi.org/10.1016/j.matlet.2013.12.060
4. Belliard, F., Irvine, J.T.S. (2001). Electrochemical performance of ball-milled ZnO±SnO_2 systems as anodes in lithium-ion battery. Journal of Power Sources 97-98, 219-222. https://doi.org.10.1016/S0378-7753(01)00544-4
5. Cai, Z., Ou, Y., Wang, J., Xiao, R., Fu, L., Yuan, Z., Zhan, R., Sun, Y. (2020). Chemically resistant Cu–Zn/Zn composite anode for long cycling aqueous batteries. *Energy Storage Materials* 27, 205–211. https://doi.org/10.1016/j.ensm.2020.01.032
6. Chou, H.S., Yang, K.Di, Xiao, S.H., Patil, R.A., Lai, C.C., Vincent Yeh, W.C., Ho, C.H., Liou, Y., Ma, Y.R. (2019). Temperature-dependent ultraviolet photoluminescence in hierarchical Zn, ZnO and ZnO/Zn nanostructures. *Nanoscale* 11(28), 13385–13396. https://doi.org/10.1039/c9nr05235f
7. Ding, Y., Sun, J., Liu, X. (2019). Carbon-decorated flower-like ZnO as high-performance anode materials for Li-ion batteries. *Ionics* 25(9), 4129–4136. https://doi.org/10.1007/s11581-019-02981-y

8. Gachot, G., Grugeon, S., Armand, M., Pilard, S., Guenot, P., Tarascon, J. M., Laruelle, S. (2008). Deciphering the multi-step degradation mechanisms of carbonate-based electrolyte in Li batteries. *Journal of Power Sources* 178(1), 409–421. https://doi.org/10.1016/j.jpowsour.2007.11.110
9. Ghosh, M., Raychaudhuri, A.K. (2008). Ionic environment control of visible photoluminescence from ZnO nanoparticles. *Applied Physics Letters* 93(12). https://doi.org/10.1063/1.2987479
10. Hao, X.P., Xu, Z., Li, C.Y., Hong, W., Zheng, Q., Wu, Z.L. (2020). Kirigami-Design-Enabled Hydrogel Multimorphs with Application as a Multistate Switch. *Advanced Materials* 32(22). https://doi.org/10.1002/adma.202000781
11. Huang, X.H., Xia, X.H., Yuan, Y.F., Zhou, F. (2011). Porous ZnO nanosheets grown on copper substrates as anodes for lithium ion batteries. *Electrochimica Acta* 56(14), 4960–4965. https://doi.org/10.1016/j.electacta.2011.03.129
12. Issatayev, N., Abdumutaliyeva, D., Tashenov, Y., Yeskozha, D., Seipiyev, A., Bakenov, Z., Nurpeissova, A. (2024). Three-dimensional carbon coated and high mass-loaded NiO@Ni foam anode with high specific capacity for lithium ion batteries. *RSC Advances* 14(54), 40069–40076. https://doi.org/10.1039/d4ra07119k
13. Issatayev, N., Adylkhanova, A., Salah, M., Bakenov, Z., Kalimuldina, G. (2024). Room temperature growth of NiS hierarchical nanoflowers on the flexible electrode surface as a cathode for lithium-ion batteries. *Materials Letters* 354. https://doi.org/10.1016/j.matlet.2023.135341
14. Issatayev, N., Nuspeissova, A., Kalimuldina, G., Bakenov, Z. (2021). Three-dimensional foam-type current collectors for rechargeable batteries: A short review. *Journal of Power Sources Advances* 10. https://doi.org/10.1016/j.powera.2021.100065
15. Khac, V., Bui, H., Pham, T.N., Hur, J., Lee, Y.-C., Bui, V.K.H., Pham, T.N., Hur, J., Lee, Y., Julien, C.M. (2021). Review of ZnO Binary and Ternary Composite Anodes for Lithium-Ion Batteries. https://doi.org/10.3390/nano
16. Kumar, K.K., Ravi, M., Pavani, Y., Bhavani, S., Sharma, A.K., Narasimha Rao, V.V.R. (2014). Investigations on PEO/PVP/NaBr complexed polymer blend electrolytes for electrochemical cell applications. *Journal of Membrane Science* 454, 200–211. https://doi.org/10.1016/j.memsci.2013.12.022
17. Li, N., Jin, S.X., Liao, Q.Y., Wang, C.X. (2014). ZnO anchored on vertically aligned graphene: Binder-free anode materials for lithium-ion batteries. *ACS Applied Materials and Interfaces* 6(23), 20590–20596. https://doi.org/10.1021/am507046k
18. Lin, J.H., Huang, Y.J., Su, Y.P., Liu, C.A., Devan, R.S., Ho, C.H., Wang, Y.P., Lee, H.W., Chang, C.M., Liou, Y., Ma, Y.R. (2012). Room-temperature wide-range photoluminescence and semiconducting characteristics of two-dimensional pure metallic Zn nanoplates. *RSC Advances* 2(5), 2123–2127. https://doi.org/10.1039/c2ra00972b
19. Liu, J., Li, Y., Huang, X., Li, G., Li, Z. (2008). Layered double hydroxide nano- and microstructures grown directly on metal substrates and their calcined products for application as Li-ion battery electrodes. *Advanced Functional Materials* 18(9), 1448–1458. https://doi.org/10.1002/adfm.200701383
20. Liu, Y., Zhu, Y., Cui, Y. (2019). Challenges and opportunities towards fast-charging battery materials. *Nature Energy* 4(7), 540–550. https://doi.org/10.1038/s41560-019-0405-3
21. Pramanik, S., Das, S., Karmakar, R., Irsad Ali, S., Mukherjee, S., Dey, S., Chandra Mandal, A., Meikap, A.K., Kuiri, P.K. (2023). Enhancement of UV luminescence in Zn/ZnO nanocomposites synthesized by controlled thermal oxidation of Zn nano-octahedrals. *Journal of Luminescence* 257. https://doi.org/10.1016/j.jlumin.2023.119746
22. Rahdar, A., Aliahmad, M., Azizi, Y. (2015). NiO Nanoparticles: Synthesis and Characterization. *JNS* 5.
23. Shen, X., Mu, D., Chen, S., Wu, B., Wu, F. (2013). Enhanced electrochemical performance of ZnO-loaded/porous carbon composite as anode materials for lithium ion batteries. *ACS Applied Materials and Interfaces* 5(8), 3118–3125. https://doi.org/10.1021/am400020n

24. Song, R., Zhang, N., Dong, H., Wang, P., Ding, H., Wang, J., Li, S. (2022). Self-standing three-dimensional porous NiO/Ni anode materials for high-areal capacity lithium storage. *Materials and Design* 215. https://doi.org/10.1016/j.matdes.2022.110448
25. Srinivasa, N., Hughes, J.P., Adarakatti, P.S., Manjunatha, C., Rowley-Neale, S.J., Ashoka, S., Banks, C.E. (2021). Facile synthesis of Ni/NiO nanocomposites: The effect of Ni content in NiO upon the oxygen evolution reaction within alkaline media. *RSC Advances* 11(24), 14654–14664. https://doi.org/10.1039/d0ra10597j
26. Tarascon, J.-M., Armand, M. (2001). Issues and challenges facing rechargeable lithium batteries.
27. Thauer, E., Zakharova, G.S., Andreikov, E.I., Adam, V., Wegener, S.A., Nölke, J.H., Singer, L., Ottmann, A., Asyuda, A., Zharnikov, M., Kiselkov, D.M., Zhu, Q., Puzyrev, I.S., Podval'naya, N.V., Klingeler, R. (2021). Novel synthesis and electrochemical investigations of ZnO/C composites for lithium-ion batteries. *Journal of Materials Science* 56(23), 13227–13242. https://doi.org/10.1007/s10853-021-06125-4
28. Tleukenov, Y.T., Kalimuldina, G., Arinova, A., Issatayev, N., Bakenov, Z., Nurpeissova, A. (2022). Polyacrylonitrile-Polyvinyl Alcohol-Based Composite Gel-Polymer Electrolyte for All-Solid-State Lithium-Ion Batteries. *Polymers* 14(23). https://doi.org/10.3390/polym14235327
29. Wang, X., Wang, Y., Wu, M., Fang, R., Yang, X., Wang, D.W. (2022). Ultrasonication-assisted fabrication of porous ZnO@C nanoplates for lithium-ion batteries. *Microstructures* 2(3). https://doi.org/10.20517/microstructures.2022.11
30. Zhang, X.Q., Cheng, X.B., Chen, X., Yan, C., Zhang, Q. (2017). Fluoroethylene Carbonate Additives to Render Uniform Li Deposits in Lithium Metal Batteries. *Advanced Functional Materials* 27(10). https://doi.org/10.1002/adfm.201605989

3D Zn/ZnO@C анодын алу үшін қарапайым термиялық тотығу және көміртекпен қаптау әдісі

Ержігіт Серік, Нұрболат Исатаев, Молдир Архарбекова, Жумабай Бакенов, Арайлым Нұрпейсова, Алия Муканова

Аңдатпа. Қазіргі таңда литий-иондық батареялар (LIBs) үшін жоғары өнімді және тұрақты анодтық материалдарды дамыту – өзекті ғылыми мәселелердің бірі. Бұл жұмыста термиялық тотығу және көміртектендіру әдістері арқылы Zn/ZnO негізіндегі үшөлшемді (3D) көбік тәрізді анод синтезделіп, оның беті полиэтиленоксид (PEO) арқылы көміртекпен қапталды. Электродтың құрылымы мен құрамы XRD, SEM, EDS және FTIR әдістері арқылы сипатталды. Үшөлшемді кеуекті құрылым литий иондары мен электрондардың тасымалын жақсарта отырып, көлемдік кеңеюдің әсерін азайтады. Көміртек қабаты ZnO-ның электрөткізгіштігін арттырып, цикл кезінде оның құрылымдық тұрақтылығын қамтамасыз етеді. Электрохимиялық зерттеу нәтижелері Zn/ZnO@C электродының 100 циклдан кейін 50 мА·г$^{-1}$ ток тығыздығында шамамен 380 мА·сағ·г$^{-1}$ сыйымдылықты тұрақты сақтайтынын көрсетті, ал көміртекпен қапталмаған Zn/ZnO аноды тек ~100 мА·сағ·г$^{-1}$ көрсетті. Алынған нәтижелер көміртекпен қапталған Zn/ZnO көбік анодтарының болашақ жоғары өнімді литий-иондық батареялар үшін перспективалы материал екенін дәлелдейді.

Түйін сөздер: литий-ионды батареялар; электрод материалдары; энергия сақтау жүйелері; электрохимия.

Простая стратегия термического окисления и нанесения углеродного покрытия для получения 3D анода Zn/ZnO@C

Ержигит Серик, Нурболат Исатаев, Молдир Архарбекова, Жумабай Бакенов, Арайлым Нурпейсова, Алия Муканова

Аннотация: В настоящее время разработка высокоэффективных и стабильных анодных материалов для литий-ионных батарей (LIBs) является актуальной научной задачей. В данной работе методом термического окисления и карбонизации был синтезирован анод на основе Zn/ZnO в виде трёхмерной (3D) пористой пены, поверхность которого была покрыта углеродом с использованием полиэтиленоксида (PEO) в качестве прекурсора. Структура и состав электрода были охарактеризованы методами XRD, SEM, EDS и FTIR. Трёхмерная пористая архитектура способствует улучшенному переносу литиевых ионов и электронов, а также снижает влияние объёмного расширения. Углеродное покрытие повышает электропроводность ZnO и обеспечивает структурную стабильность материала в процессе циклирования. Электрохимические испытания показали, что электрод Zn/ZnO@C сохраняет стабильную удельную ёмкость около 380 мА·ч/г после 100 циклов при плотности тока 50 мА/г, тогда как необработанный электрод Zn/ZnO продемонстрировал лишь ~100 мА·ч/г. Полученные результаты подтверждают перспективность пеноматериалов Zn/ZnO с углеродным покрытием в качестве анодных материалов для литий-ионных батарей нового поколения.

Ключевые слова: литий-ионные батареи; электродные материалы; системы накопления энергии; электрохимия.